Available online www.jocpr.com

Journal of Chemical and Pharmaceutical Research, 2015, 7(2):446-453

Research Article

ISSN : 0975-7384
CODEN(USA) : JCPRC5

Investigations on the structural and electrical properties of 4-chloro-n-methyl 4-stilbazolium tosylate

Amirdha Sher Gill

Department of Physics, Sathyabama University, Chennai, Tamil Nadu, India

---

ABSTRACT

A new optical material 4-chloro -N- methyl 4-stilbazolium tosylate, a new derivative of the stilbazolium tosylate family has been synthesized and transparent single crystals were grown by slow solvent evaporation technique. The grown crystals were tested for structural and electrical characterization such as single, powder and high resolution X-ray diffraction and dielectric measurements. The crystal system and lattice parameters were found from single crystal X-ray diffraction. Crystalline perfection has been found using X-ray rocking curve. Formations of defects were analyzed from etching studies. The dielectric constant, dielectric loss and dielectric impedance as a function of frequency and temperature were studied from the LCZ analysis.

Keywords: A. optical materials; B. chemical synthesis; C. X-ray diffraction; D. crystal structure; D. dielectric properties

---

INTRODUCTION

The organic compounds have been found to have potential to exceed inorganic compounds due to their practical applications such as optical communication, optical information processing, optical disk data storage, laser fusion reactions, laser remote sensing, color display and medical diagnostics [1]. Many organic compounds show good nonlinear optical (NLO) property due to the presence of π-conjugation systems, which helps in the molecular engineering for the tailor made applications. During recent years, stilbazolium tosylate derivatives have attracted a great deal of attention for their unique π-bonds showing good optical nonlinearities and transparency [2-5]. Recently, new derivatives of stilbazolium tosylate family crystals with high SHG and laser damage threshold have been reported [6-10]. More recently, we reported the synthesis, crystal growth and some properties of 4-chloro N-methyl 4-stilbazolium tosylate (CMST), which is a new derivative in the stilbazolium tosylate family with NLO property and one of the new organic material [11]. In the present work, we report here the structural and dielectric properties of the title crystal. The surfaces of the grown crystals were analyzed with chemical etching.

EXPERIMENTAL SECTION

MATERIAL SYNTHESIS

The title compound was synthesized by the condensation of 4-methyl-N-methyl pyridinium tosylate, which was prepared from 4-picoline (C_6H_7N), methyl p-toluene sulfonate ($C_8H_{10}O_3S$) and 4-chloro benzaldehyde (C_7H_5ClO) in the presence of piperidine as catalyst [11]. Transparent crystals of size 10 mm x 6 mm x 2 mm were obtained after successive recrystallization processes.

2. Instruments for Characterization

The quality of the grown crystal was analyzed by different instrumentation methods such as single crystal and high resolution X-ray diffraction, and dielectric studies. Single crystal X-ray diffraction analysis was performed by means of Bruker Smart Apex Instrument with Mo Kα radiation of wavelength 0.7170 Å at 298 K. The crystalline perfection of the grown single crystals was characterized by HRXRD by employing a multicrystal X-ray diffractometer developed at NPL [12]. The well-collimated and monochromated MoKα_1 beam obtained from the three monochromator Si crystals set in dispersive (+,-,-) configuration has been used as the exploring X-ray beam. The specimen crystal is aligned in the (+,-,-,+) configuration. Due to dispersive configuration, though the lattice constant of the monochromator crystal and the specimen are different, the unwanted dispersion broadening in the diffraction curve (DC) of the specimen crystal is insignificant. The specimen can be rotated about the vertical axis, which is perpendicular to the plane of diffraction, with minimum angular interval of 0.4 arc s. The DC was recorded by the so-called ω scan wherein the detector was kept at the same angular position $2\theta_B$ with wide opening for its slit. All the surfaces of the crystal were etched and examined for the presence of defects by an optical microscope. The dielectric study for the single crystal was carried out using the instrument, HIOKI 3532- 50 LCR HITESTER for the frequency range 50 Hz to 5 MHz

3.1. Single crystal X-ray diffractometry

Single crystal X-ray diffraction analysis was used to confirm the molecular and crystal structure of the grown crystal. **Figure 1** shows the molecular structure with the numbering scheme of the title material and the displacement ellipsoids are drawn at the 50% probability level. The structure was solved by direct methods, refined and all further calculations were carried out using the programme SHELXS-97 [13]. All atoms except hydrogen atoms were refined anisotropically using weighted full-matrix least-squares on F^2. Hydrogen atoms were placed at calculated positions on the basis of stereo-chemical considerations and refined according to the riding model. From the analysis, the crystal system was found to be monoclinic with cell parameters a = 9.041(3) Å, b = 6.437(2) Å, c = 33.788(5) Å, β = 94.31(3) ° and volume = 1960.9 Å^3. **Figure 2** reveals the packing diagram of the crystal viewed down the b-axis. CCDC772964 contains the supplementary crystallographic data for CMST and this data can be obtained free of charge from the Cambridge Crystallographic Data Centre via www.ccdc.cam.ac.uk/data_request/cif [14].

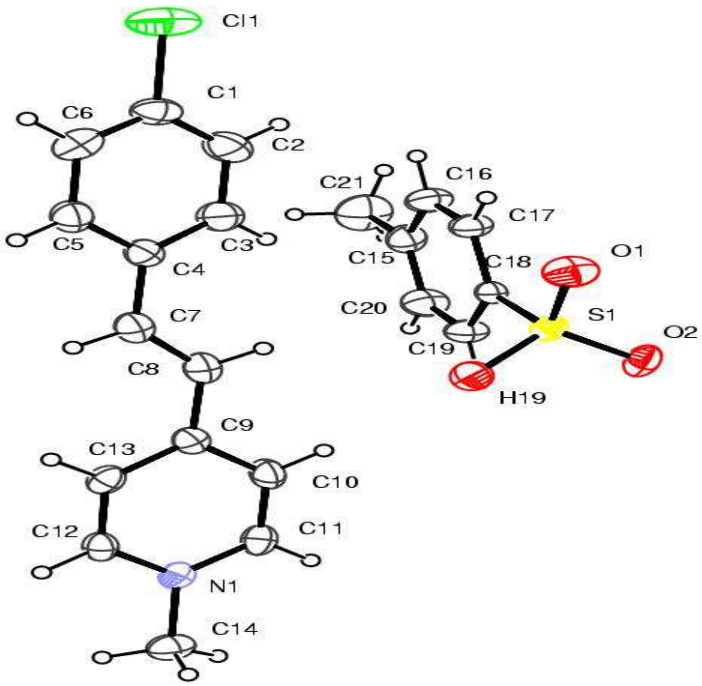

Figure 1. Structure of the title crystal with numbering scheme

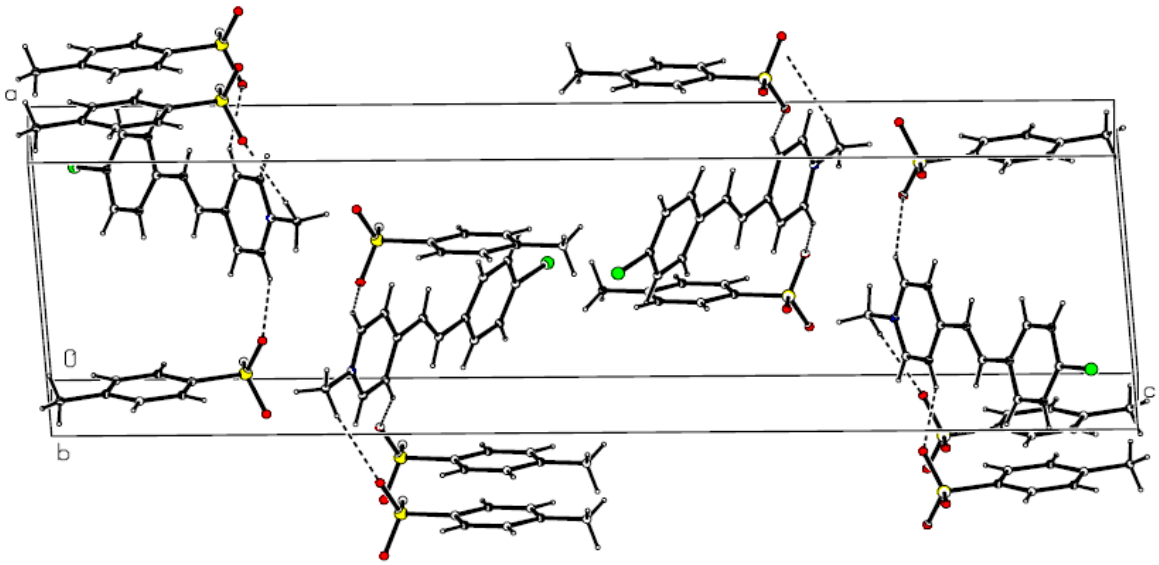

Figure 2. Crystal Packing diagram viewed down the b- axis

3.2. Multicrystal X-ray diffractometry

The specimen surface was prepared by lapping and polishing before recording the diffraction curve, and then it was chemically etched by a non preferential chemical etchant mixed with water and acetone in 1:2 ratio. **Figure 3** shows the high-resolution diffraction curve (DC) recorded for a typical CMST single crystal specimen using (001) diffracting planes in symmetrical Bragg geometry by employing the multicrystal X-ray diffractometer with MoKα_1 radiation. The solid line (convoluted curve) is well fitted with the experimental points represented by the filled circles. On deconvolution of the diffraction curve, it is clear that the curve contains two additional peaks, which are 32 and 53 arc s away from the central peak. These two additional peaks correspond to two internal structural very low angle (tilt angle $\leq$ 1 arc min) grain boundaries [15] whose tilt angles (misorientation angle between the two crystalline regions on both sides of the structural grain boundary) are 32 and 53 arc s from the main crystalline block.

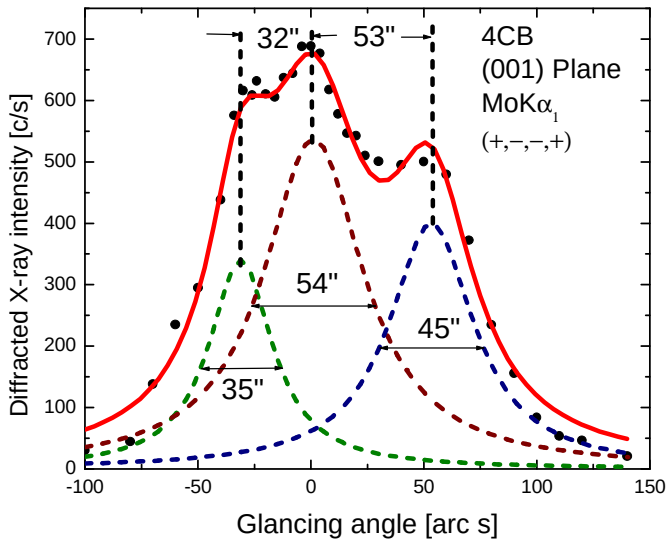

Figure 3. High-resolution diffraction curve recorded for the specimen crystal

The FWHM (full width at half maximum) of the main peak and the very low angle boundaries are 54 and 35 & 45 arc s respectively. Though the specimen contains low angle boundaries, the relatively low angular spread of around 250 arc s of the diffraction curve shows that the crystalline perfection is reasonably good. The affect of such low angle boundaries may not be very significant in many applications, but for application like phase matching, it is better to know these minute details regarding crystalline perfection.

3.3. Etching studies

The etching studies were carried out in order to know the quality of the grown crystal. The chemical etching is helpful for the identification of the structural defects present in the crystals, which develops as growth hillocks, etch pits and grain boundaries on the crystal surface [16]. All the surfaces of the CMST crystal was polished using a velvet cloth, and then etched using the solvents for 10 s and again for 30 s. Though methanol, ethanol and acetone were used as etchant, methanol, being used as the solvent of crystallization, was found as the perfect etchant as observed by the optical microscope. For the purpose of comparison the surfaces were observed before (fig. 4a) the application of the etchant. It shows the growth surface as rough faces. Figures 4 b shows the optical micrograph of the same surface etched for 10 s. When the surfaces were etched for 10 s the surface has become smooth without any rough edges and we can see some pits present on the surface. Again etching for another 20 s the same surface washes out all the remaining pits and now the surface is free from any defects as seen in the fig. 4c.

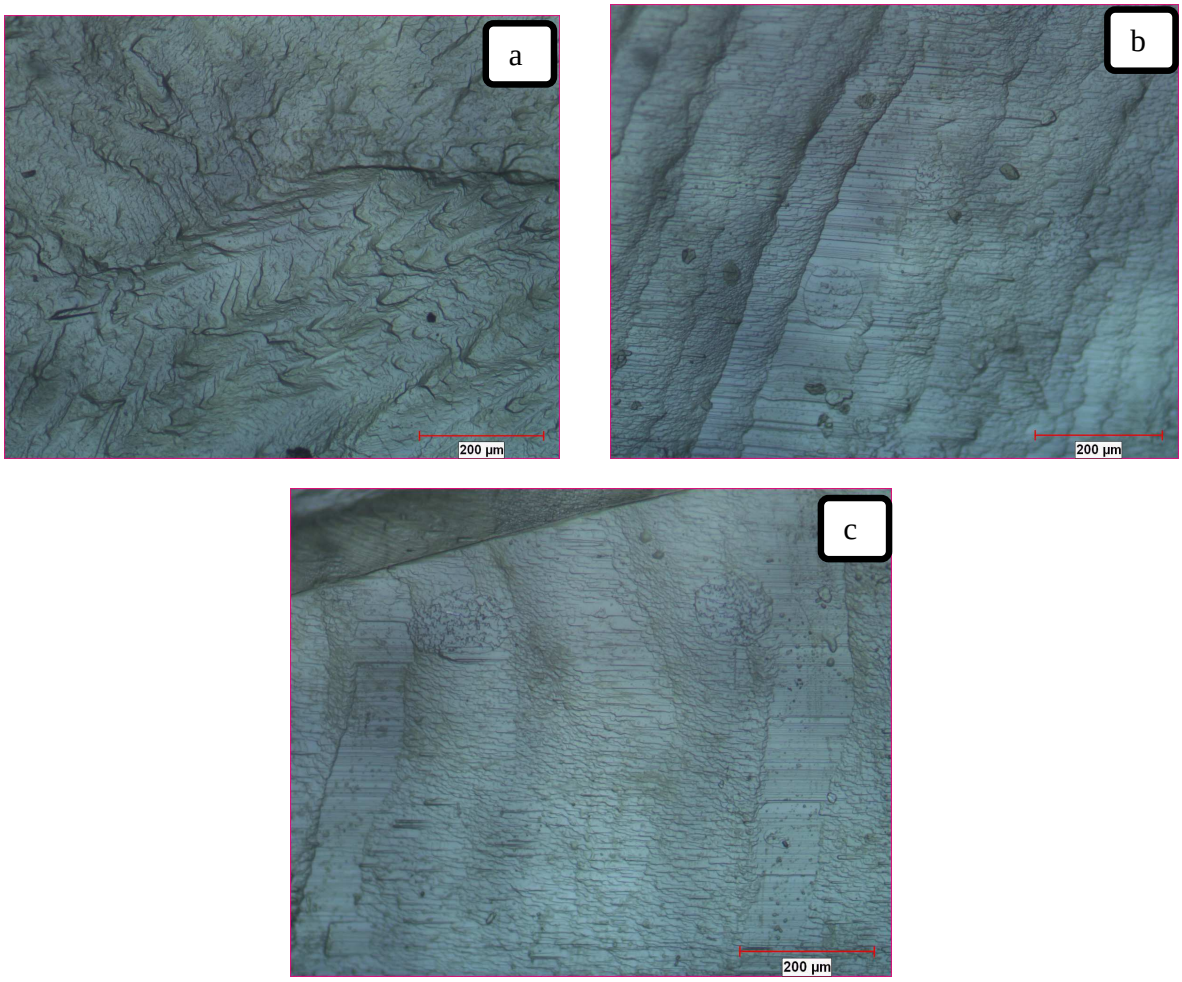

Figure. 4. Optical micrograph of the (a) crystal before applying etchant (b) after 10 s etching (c) after 30 s of etching

3.4. Dielectric studies

A sample of dimension $6\times5\times1mm^3$ was used for measurements after coating electronic grade silver paste on the opposite faces of the crystal. It was placed between the two copper electrodes and thus a parallel plate capacitor was

formed. The capacitance (C), conductance (G), impedance (Z) and dielectric loss (D) of the sample were measured using LCZ meter in the frequency range 50 Hz to 5 MHz by varying the temperature from room temperature to 200 ºC in steps of 25 ºC.

The dielectric constant (ε_r) is calculated from the following equation, $\varepsilon_r = Ct/\varepsilon_o A$, where ε_o is the permittivity of free space, t is the thickness of the sample and A is the area of cross section of the sample. **Figure 5** shows the plot of dielectric constant versus frequency. Generally, the dielectric constant decreases with increase in frequency and reaches a constant value, depending on the fact that beyond a certain frequency of the electric field, the dipole does not follow the alternating field. The dielectric constant has high values in the lower frequency region and then it decreases with the increase of frequency. The dielectric constant has a high value of 46 at 50 Hz for 200 ºC and decreases to 3 around 5 MHz for the temperature 50 ºC. The very high value of ε_r at low frequencies may be due to the presence of all the four polarizations namely, space charge, orientational, electronic and ionic polarization, and its low value at higher frequencies may be due to the loss of significance of these polarizations gradually and only space charge polarization is active at lower frequencies for high temperatures and indicates the perfection of the crystals [17]. The imaginary part of dielectric constant is shown in **fig. 6.** The ε'' decreases as the frequency is increased gradually and it approaches zero irrespective of temperature. This behavior is common in the case of ionic systems.

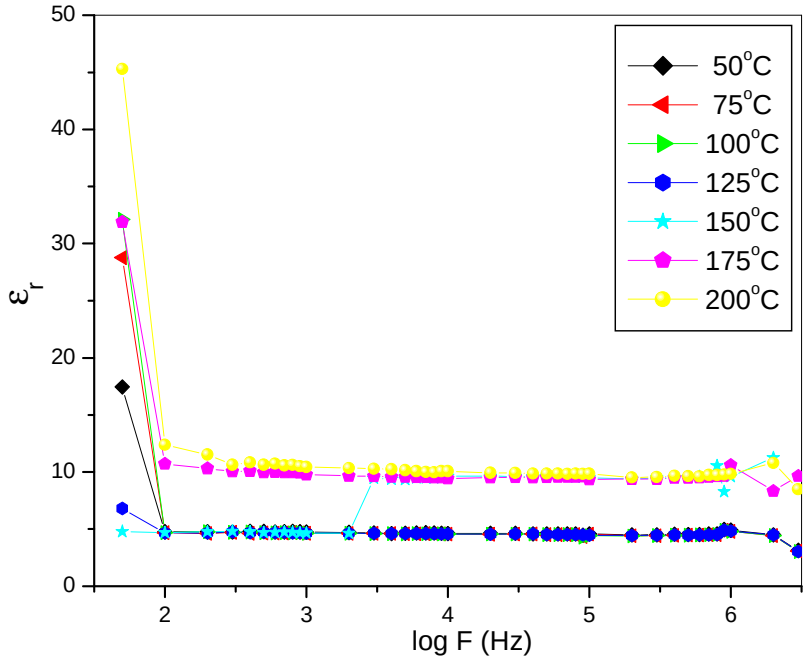

Figure. 5. The plot of real part of dielectric constant versus frequency for various temperatures

The dielectric loss, tan δ is also studied as a function of frequency by varying the temperature and is shown in **fig.7 and 8**. These curves suggest that the dielectric loss is strongly dependent on the frequency of the applied field similar to that of dielectric constant. At low frequencies, the dielectric loss was found to be large at room temperature and at 200 ºC. For all other temperatures, the dielectric loss is almost zero as seen in fig.7. The measure of low dielectric loss at higher frequencies is due to dipole rotation. At high frequencies, the orientation polarization ceases and hence, the energy need not be spent to rotate dipoles. Low value of dielectric loss indicates that very low defects which is in tune with the etching results. It is also observed that dielectric loss depend on the temperature and increases slightly with an increase of temperature (fig.8). The changes of εr and tan δ as a function of frequency may be considered as a normal behavior of dielectric [18]. Fig. 9 shows the Nyquists diagram between the imaginary parts of impedance (Z) versus real part of impedance. It is revealed from the semicircle plot that the behavior of the electrical response obeys cole – cole formulation.

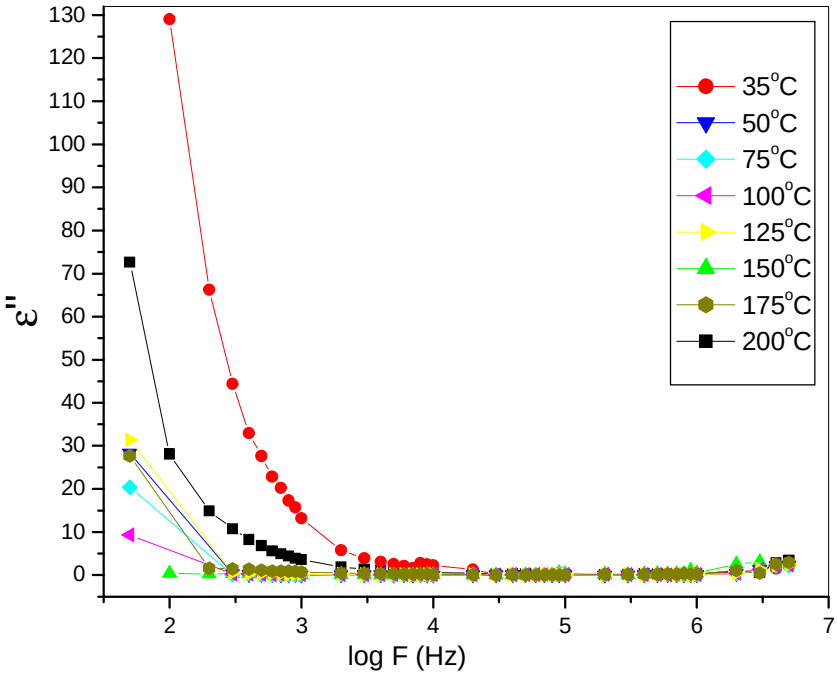

Figure. 6. The plot of imaginary part of dielectric constant versus frequency for various temperatures

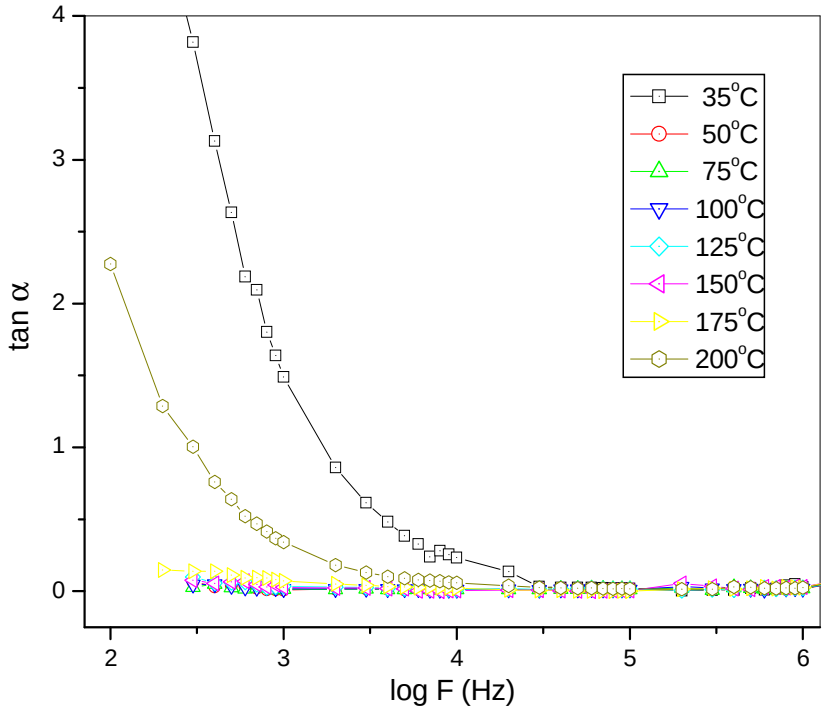

Figure. 7. The graph of dielectric loss versus log frequency for various temperatures

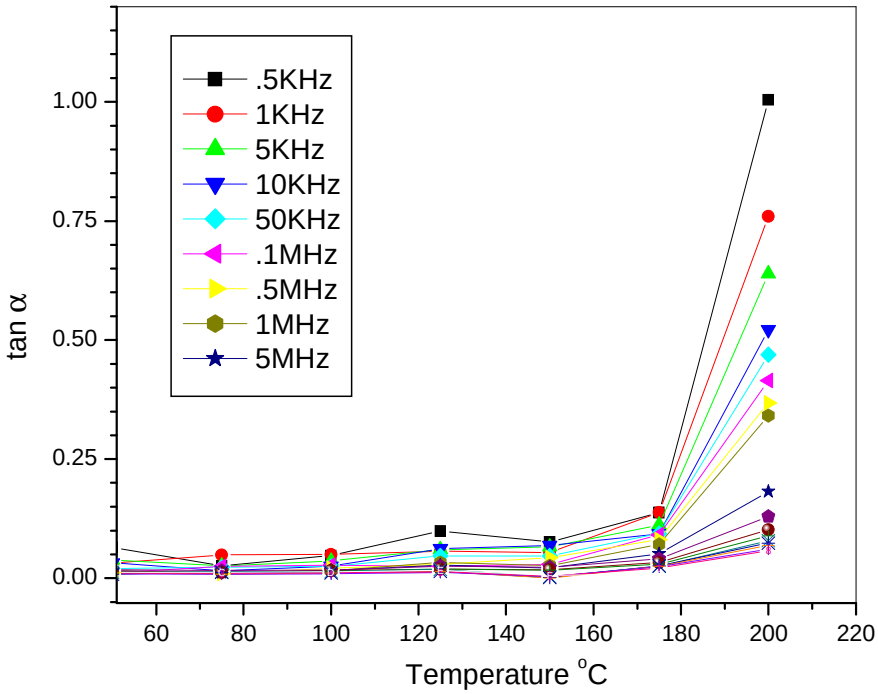

Figure. 8. The graph of dielectric loss versus temperature for various frequencies

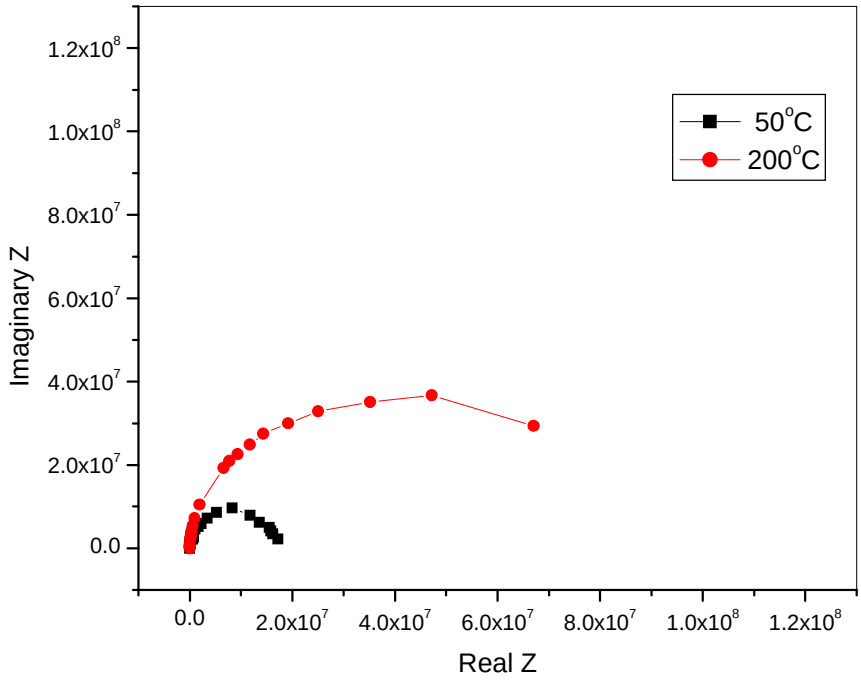

Figure. 9. Nyquists diagram between the real and imaginary parts of impedance

CONCLUSION

Relatively large size crystals of CMST with good optical grade were grown by slow solvent evaporation technique. The single crystal XRD studies confirm that the grown crystal belongs to triclinic system. Crystalline perfection of the grown crystal was examined through X-ray rocking curve measurements. Defect evaluation of the crystals was analyzed by chemical etching analysis. The dielectric studies prove that the sample has low dielectric constant and low dielectric loss at high frequency and hence it will be suitable material for electro-optic applications.

REFERENCES

[1] SR Marder, JW Perry, WP Schaefer, *Science*, **1989**, 245, 626-628.
[2] Min Ju Cho, Dong Hoon Choi, Philip A Sullivan, Andrew JP Akelaitis, Larry R Dalton, *Prog. Polym. Sci*. **2008,** 33, 1013-1058.
[3] A Sugita, K Yanagi, K Kuroyanagi, H Takahashi, S Aoshima, Y Tsuchiya, S Tasaka, H Hashimoto, *Chem. Phys*. Lett. **2003,** 382, 693-698.
[4] B Ruiz, Z Yang, V Gramlich, M Jazbinsek, P Gunter, *J. Mater. Chem*. **2006,** 16, 2839-2842.
[5] R Jerald Vijay, N Melikechi, T Rajesh Kumar, Joe GM. Jesudurai, P Sagayaraj, *J. Cryst. Growth* **2010,** 312, 420-425.
[6] Benjamin J Coe, Simon P Foxon, Elizabeth C Harper, James A. Harris, M. Helliwell, J. Raftery, I. Asselberghs, K Clays, E Franz, Bruce S Brunschwig, AG Fitch, *Dyes Pigm.* **2009**, 82, 171-186.
[7] T Matsukawa, Y Takahashi, R. Miyabara, H. Koga, H. Umezawa, I. Kawayama, M. Yoshimura, S. Okada, M. Tonouchi, Y. Kitaoka, Y. Mori, T Sasaki, *J. Cryst. Growth*, **2009,** 311, 568-571.
[8] K Jagannathan, S Kalainathan, G Bhagavannarayana, *Spectrochim. Acta.* A, **2009,** 73, 79-83.
[9] Amirdha Sher Gill, S. Kalainathan, G. Bhagavannarayana, *Mater Lett*. **2010**, 64, 1989-91.
[10] Amirdha Sher Gill, S Kalainathan, *J.Phys. Chem. Solids*, **2011**, 72, 961-967.
[11] Amirdha Sher Gill, S Kalainathan, *Arch. Phys. Res*., **2010**, 1(4), 41-47.
[12] Krishan Lal and G Bhagavannarayana, *J. Appl. Crystallogr.* **1989**, 22, 209-215.
[13] GM Sheldrick, *Acta Cryst. A*, **2008,** 64, 112-122.
[14] Cambridge Crystallographic Data Center (CCDC), 12 Union Road, Cambridge CB2 1EZ, UK; fax: +44(0)1223-336033.
[15] G Bhagavannarayana, RV Ananthamurthy, GC Budakoti, B Kumar, KS Bartwal, *J. Appl. Crystallogr*. **2005**, 38, 768-771.
[16] S Arjunan, R Mohan Kumar, R Mohan, R Jayavel, *Mater. Res. Bull*. **2008,** 43, 2018-2025.
[17] TC Sabari Girisun, S Dhanuskodi, *Mater. Res. Bull*. **2010**, 45, 88-91.
[18] P Selvarajan, J Glorium Arulraj, S Perumal, *Physica B* **2010,** 405, 738–743.